

## A WAVELET-BASED SCALE-DEPENDENT ANALYSIS OF LAGRANGIAN AND EULERIAN ACCELERATIONS IN TURBULENT STRATIFIED SHEAR FLOW

**Frank G. Jacobitz**

Department of Mechanical Engineering  
 University of San Diego  
 5998 Alcalá Park, San Diego, CA 92110, USA  
 jacobitz@sandiego.edu

**Kai Schneider**

Aix Marseille Univ, CNRS, Centrale Marseille, I2M  
 39 rue Joliot-Curie, 13453 Marseille Cedex 13, France  
 kai.schneider@univ-amu.fr

### ABSTRACT

The correlations of Lagrangian and Eulerian accelerations are studied in homogeneous turbulence with uniform shear and stable stratification using direct numerical simulations. The Richardson number is varied from  $Ri = 0$ , corresponding to unstratified shear flow, to  $Ri = 1$ , corresponding to strongly stratified shear flow. The correlations between the accelerations are observed to increase with increasing  $Ri$ . Using a wavelet-based scale decomposition of the accelerations, their correlations at different scales of motion are investigated. The accelerations are found to be strongly correlated at large scales of motion, but their correlations decrease with decreasing scale of the turbulent motion. A similar analysis is performed for the Lagrangian and Eulerian time-rates of change of the fluctuating density. Again, the correlations between the time-rates of change are observed to increase with increasing Richardson number and to decrease with decreasing scale of motion.

### INTRODUCTION

The Lagrangian and Eulerian dynamics of homogeneous turbulent stratified shear flow with constant vertical stratification rate  $S_\rho = \partial\rho/\partial y$  and constant vertical shear rate  $S = \partial U/\partial y$  are studied using direct numerical simulations. The consideration of this prototypical flow is motivated by the importance of an understanding of turbulent transport and mixing processes of natural and anthropogenic substances in the geophysical environment. Homogeneous turbulent stratified shear has been investigated extensively in the past, including the experimental work by Komori *et al.* (1983), Rohr *et al.* (1988), and Keller & Van Atta (2000), as well as numerical simulations by Gerz *et al.* (1989), Holt *et al.* (1992), Jacobitz *et al.* (1997), and Jacobitz (2002). An analysis of the flow using linear theory has been performed by Hanazaki & Hunt (2004).

The Lagrangian acceleration properties of a fluid particle in turbulent motion was originally considered by Heisenberg (1948). More recent studies on this topic range

from theoretical investigations (e.g. Tsinober, 2001) to applications such as the modeling of particle dispersion (e.g. Pope, 1994). Again, the work was carried out using both experimental (e.g. La Porta *et al.*, 2001) as well as computational (e.g. Yeung, 2002; Toschi & Bodenschatz, 2009) approaches.

The goal of the present study is to extend the work reported in Jacobitz *et al.* (2015) through an investigation of the correlations between Lagrangian and Eulerian accelerations in homogeneous turbulent stratified shear flows using direct numerical simulations. In the following, the simulation approach is introduced and results on the correlations of Lagrangian and Eulerian accelerations are presented.

### APPROACH

In this section, the numerical approach and the wavelet-based scale-dependent decomposition are introduced.

### Equations of Motion

This study of homogeneous turbulent stratified shear flow is based on the incompressible Navier–Stokes equations for the fluctuating velocity and an advection-diffusion equation for the fluctuating density.

$$\nabla \cdot \mathbf{u} = 0 \quad (1)$$

$$\frac{\partial \mathbf{u}}{\partial t} + \mathbf{u} \cdot \nabla \mathbf{u} + S_y \frac{\partial \mathbf{u}}{\partial x} + S_v \mathbf{e}_x = -\frac{1}{\rho_0} \nabla p - \frac{g}{\rho_0} \rho \mathbf{e}_y + \nu \nabla^2 \mathbf{u} \quad (2)$$

$$\frac{\partial \rho}{\partial t} + \mathbf{u} \cdot \nabla \rho + S_\rho v = \alpha \nabla^2 \rho \quad (3)$$

Here,  $\mathbf{u}$  is the fluctuating velocity,  $p$  the fluctuating pressure,  $\rho$  the fluctuating density,  $\nu$  the viscosity, and  $\alpha$  the

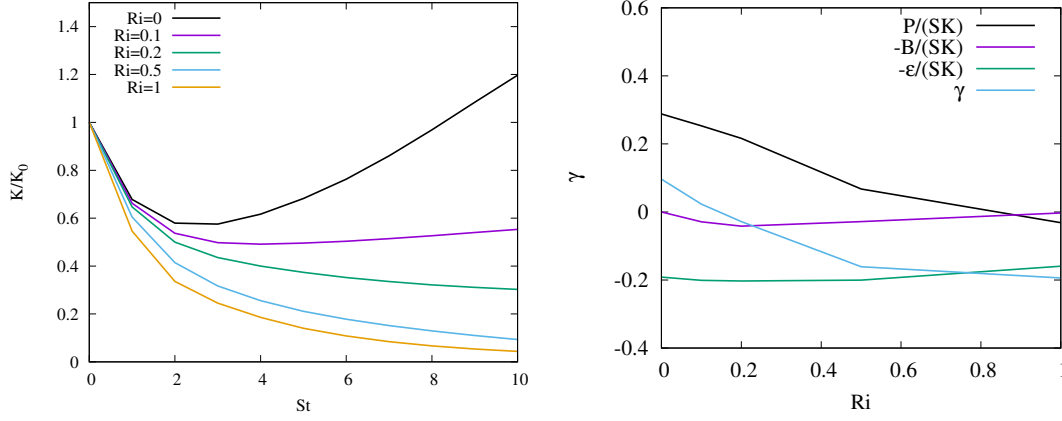


Figure 1. Evolution of the turbulent kinetic energy  $K$  in nondimensional time  $St$  (left) and dependence of the normalized production rate  $P/(SK)$ , buoyancy flux  $B/(SK)$ , and dissipation rate  $\epsilon/(SK)$  on the Richardson number at  $St = 10$  (right).

scalar diffusion. The equations of motion are transformed into a frame of reference moving with the mean velocity (see Rogallo, 1981). This transformation enables the application of periodic boundary conditions for the fluctuating components of velocity and density. A spectral collocation method is used for the spatial discretization and the solution is advanced in time with a fourth-order Runge–Kutta scheme.

The simulations are performed on a parallel computer using  $512 \times 512 \times 512$  grid points. The primary nondimensional parameter, the Richardson number  $Ri = N^2/S^2$ , where  $N$  is the Brunt–Väisälä frequency with  $N^2 = -g/\rho_0 S \rho$ , is varied from  $Ri = 0$ , corresponding to unstratified shear flow, to  $Ri = 10$ , corresponding to strongly stratified shear flow. The initial conditions are taken from a separate simulation of isotropic turbulence without density fluctuations, which was allowed to develop for approximately one eddy turnover time. The initial values of the Taylor-microscale Reynolds number  $Re_\lambda = 89$  and the shear number  $SK/\epsilon = 2$  are fixed.

The Lagrangian and Eulerian accelerations are defined as

$$\mathbf{a}_L = \frac{\partial \mathbf{u}}{\partial t} + \mathbf{u} \cdot \nabla \mathbf{u} \quad \text{and} \quad \mathbf{a}_E = \frac{\partial \mathbf{u}}{\partial t}, \quad (4)$$

respectively. Both accelerations are computed as a volume average at a fixed time, which is an appropriate choice for homogeneous flows. The effects of shear and buoyancy are considered as external forces. The time-rates of change of fluctuating density can also be defined using Lagrangian and Eulerian approaches as

$$s_L = \frac{\partial \rho}{\partial t} + \mathbf{u} \cdot \nabla \rho \quad \text{and} \quad s_E = \frac{\partial \rho}{\partial t}, \quad (5)$$

respectively.

### Wavelet-Based Scale-Dependent Decomposition

To obtain insight into the scale dependence of the statistics we decompose both accelerations into an orthogonal wavelet series. Wavelets are well localized functions

in space and in scale (see, e.g. Mallat, 1998) and different wavelet-based diagnostics, such as scale-dependent energy distribution and their spatial fluctuations, intermittency measures, e.g. scale dependent flatness and anisotropy measures have been proposed. For a review we refer the reader to Farge & Schneider (2015).

We consider a generic vector field  $\mathbf{a} = (a_1, a_2, a_3)$  at a fixed time instant and decompose each component  $a_\ell(\mathbf{x})$  into an orthogonal wavelet series,

$$a_\ell(\mathbf{x}) = \sum_{\lambda} \tilde{a}_{\lambda}^{\ell} \psi_{\lambda}(\mathbf{x}) \quad (6)$$

where the wavelet coefficients are given by the scalar product  $\tilde{a}^{\ell} = \langle a_{\ell}, \psi_{\lambda} \rangle$ . The wavelets  $\psi_{\lambda}$  with the multi-index  $\lambda = (j, \mathbf{i}, d)$  are well localized in scale  $2^{-j}$ , around position  $\mathbf{i}/2^j$ , and orientated in one of the seven directions  $d = 1, \dots, 7$ , respectively.

Reconstructing the three components  $a^{\ell}$  at scale  $2^{-j}$  by summing only over position  $\mathbf{i}$  and direction  $d$  indices in eq. (6) yields the acceleration at this scale,  $\mathbf{a}^j$ . By construction we have  $\mathbf{a} = \sum_j \mathbf{a}^j$ , where the  $\mathbf{a}^j$  are mutually orthogonal.

## RESULTS

In this section, results on the general flow evolution, the correlations of Lagrangian and Eulerian accelerations, and the correlations of the corresponding Lagrangian and Eulerian time-rates of change of fluctuating density are presented.

### Turbulence Evolution

In order to provide a context for the present study, the energetics of the flow is briefly discussed. More details on turbulent stratified shear flows can be found in Jacobitz *et al.* (1997) and Jacobitz (2002).

Figure 1 (left) shows the evolution of the turbulent kinetic energy normalized by its initial value  $K/K_0$ . All cases result in an initial decay phase due to the isotropic initial conditions. Then, as the Richardson number  $Ri$  is increased, the eventual evolution of the turbulent kinetic energy changes from growth to decay with a critical value of  $Ri_{cr} \approx 0.15$ .

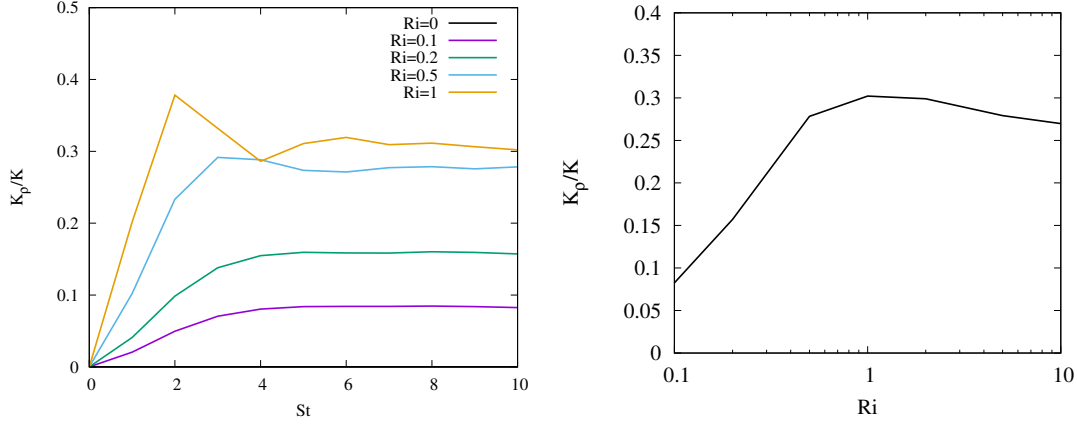


Figure 2. Evolution of the ratio of turbulent potential to kinetic energy  $K_p/K$  in nondimensional time  $St$  (left) and dependence of this ratio on the Richardson number at  $St = 10$  (right).

The normalized transport equation for the turbulent kinetic energy evolution can be written as:

$$\gamma = \frac{1}{SK} \frac{dK}{dt} = \frac{P}{SK} - \frac{B}{SK} - \frac{\varepsilon}{SK} \quad (7)$$

Here,  $\gamma$  is the growth rate of the turbulent kinetic energy,  $P/(SK)$  is the normalized production term with  $P = -\overline{S\bar{u}_1\bar{u}_2}$ ,  $B/(SK)$  is the normalized buoyancy flux with  $B = g/\rho_0\overline{u_2\bar{\rho}}$ , and  $\varepsilon/(SK)$  is the normalized dissipation rate with  $\varepsilon = \nu\overline{\partial u_j/\partial x_k\partial u_j/\partial x_k}$ .

Figure 1 (right) shows the dependence of  $P/(SK)$ ,  $B/(SK)$ ,  $\varepsilon/(SK)$ , and  $\gamma$  on the Richardson number  $Ri$  at nondimensional time  $St = 10$ . The normalized production rate  $P/(SK)$  decreases with increasing Richardson number  $Ri$  and it assumes a slightly negative value for large  $Ri$  cases, indicating a counter-gradient flux. The normalized buoyancy flux  $B/(SK)$  remains relatively small and it converts kinetic to potential energy for most of the  $Ri$  range. The normalized dissipation rate  $\varepsilon/(SK)$  remains relatively unaffected by the  $Ri$  variation. The growth rate  $\gamma$ , follows the trend of the normalized production rate  $P/(SK)$ , offset by the contributions of  $B/(SK)$  and  $\varepsilon/(SK)$ . Note that positive values of  $\gamma$  correspond to a growth of  $K$ , which a negative value of  $\gamma$  indicates decay of the turbulent kinetic energy.

The evolution of the ratio of potential to kinetic energy is given in figure 2 (left). The simulations are initialized without potential energy and a strong initial growth is observed. The ratio of potential to kinetic energy eventually reaches an approximately constant value, which still depends on the Richardson number  $Ri$ . This dependence of  $K_p/K$  on  $Ri$  at  $St = 10$  is presented in figure 2 (right). The ratio of  $K_p/K$  first increases strongly, reaches a maximum of  $K_p/K \approx 0.3$  for  $Ri \approx 1$ , and finally slightly decreases for large  $Ri$ .

### Correlation of Lagrangian and Eulerian Accelerations

The joint pdfs of Lagrangian and Eulerian accelerations are shown in figure 3 (top) for two cases with Richardson numbers  $Ri = 0.1$  (left) and  $Ri = 1$  (right) at nondimensional time  $St = 10$ . The correlation between Lagrangian and Eulerian accelerations is observed to increase with increasing  $Ri$ . In order to quantify this observation, the Pearson product-moment correlation coefficient for the

Lagrangian and Eulerian accelerations at nondimensional time  $St = 10$  is given in the first line of table 1 in dependence of the Richardson number  $Ri$ . For unstratified shear flow with  $Ri = 0$ , the Lagrangian and Eulerian accelerations are almost decorrelated with  $r = 0.0284$ . With increasing stratification strength the Pearson product-moment correlation coefficient increases monotonically and a high value of  $r = 0.9371$  is observed for  $Ri = 10$ .

Figure 3 also shows the scale-dependent joint pdfs of the Lagrangian and Eulerian accelerations for two cases with  $Ri = 0.1$  (left) and  $Ri = 1$  (right), as well as at a large scale of motion with scale index  $j = 3$  (center) and at a small scale of motion with  $j = 7$  (bottom) at nondimensional time  $St = 10$ . Consistent with the observation for the total accelerations discussed above, the correlation increases with stratification strength at the different scales shown. In addition, the correlation decreases with decreasing scale or increasing scale index  $j$ .

This observation is also shown more quantitatively using the Pearson product-moment correlation coefficient in table 1 for selected values of the scale index  $j$ . At all scales, the correlation coefficient tends to increase with increasing Richardson number  $Ri$ . Similarly, at all Richardson numbers, the correlation coefficient decreases with decreasing scale or increasing scale index  $j$ . Hence, the correlation between Lagrangian and Eulerian accelerations are found to increase with increasing Richardson number  $Ri$ , but to decrease with increasing scale index  $j$  or decreasing scale of motion.

### Correlation of Lagrangian and Eulerian Time-Rates of Change of Fluctuating Density

The joint pdfs of Lagrangian and Eulerian time-rates of change are presented in figure 4 (top) for two cases with Richardson numbers  $Ri = 0.1$  (left) and  $Ri = 1$  (right) at nondimensional time  $St = 10$ . Similarly to the correlation between Lagrangian and Eulerian accelerations, the correlation between the time-rates of change also increases with increasing  $Ri$ . However, the joint pdf for the time-rates of change differs from that of the acceleration at  $Ri = 0.1$ , because the Lagrangian time-rate of change of fluctuating density is not determined by a quadratic term in the advection-diffusion equation for fluctuating density. The Lagrangian acceleration, however, is impacted by the pressure-gradient term in the Navier–Stokes equation and the Eulerian time-

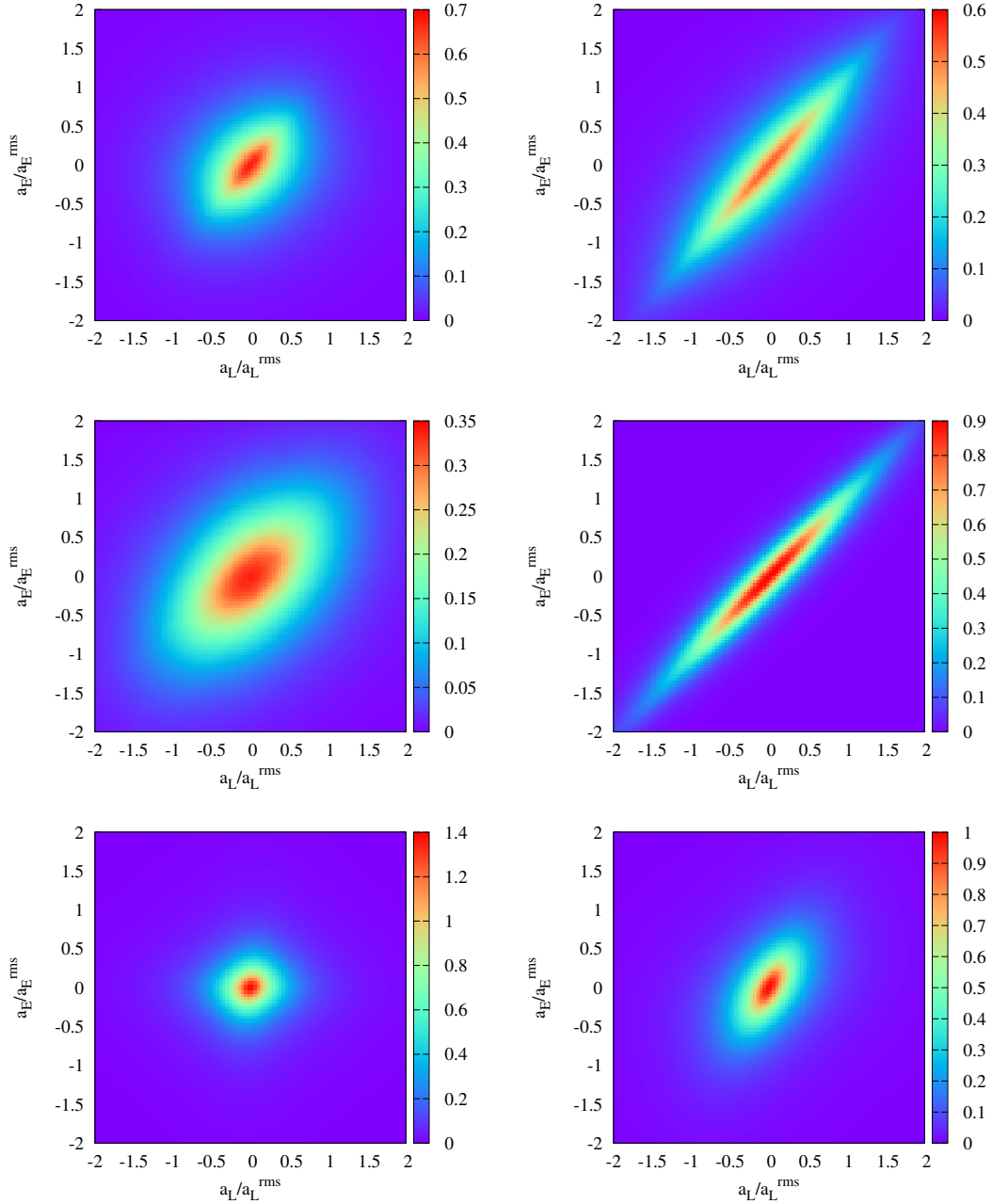


Figure 3. Joint pdfs of Lagrangian acceleration  $\mathbf{a}_L$  and Eulerian acceleration  $\mathbf{a}_E$  for Richardson numbers  $Ri = 0.1$  (left) and  $Ri = 1$  (right) for the total accelerations (top), at scale index  $j = 3$  (center), and at scale index  $j = 7$  (bottom) at nondimensional time  $St = 10$ .

rate of change as well as Eulerian acceleration are impacted by the advection terms in their respective equations. This impact is diminished at larger Richardson numbers due to a decrease of the impact of the quadratic terms. Please also see the discussion in Jacobitz *et al.* (2015).

The Pearson product-moment correlation coefficient for the Lagrangian and Eulerian time-rates of change of fluctuating density at nondimensional time  $St = 10$  is given in the first line of table 2 in dependence of the Richardson number  $Ri$ . For unstratified shear flow with  $Ri = 0$ , the density is a passive scalar and the Lagrangian and Eulerian time-rates of change are again almost decorrelated with  $r = 0.0219$ . The Pearson product-moment correlation coefficient increases with increasing Richardson number to a value of  $r = 0.9859$  for  $Ri = 10$ .

The scale-dependent joint pdfs of the Lagrangian and Eulerian time-rates of change are given in figure 4 for two cases with  $Ri = 0.1$  (left) and  $Ri = 1$  (right) as well as at a large scale of motion with scale index  $j = 3$  (center) and at a small scale of motion with  $j = 7$  (bottom) at nondimensional time  $St = 10$ . The results are similar to those obtained for the accelerations and the correlations are stronger for larger Richardson numbers and at larger scales of motion at smaller scale index  $j$ ,

The Pearson product-moment correlation coefficient of the Lagrangian and Eulerian time-rates of change of fluctuating density confirms this observation as shown in table 2 for selected values of the scale index  $j$ . For a given scale index  $j$ , the correlation coefficient increases with increasing Richardson number. For a given  $Ri$ , the correlation coefficient

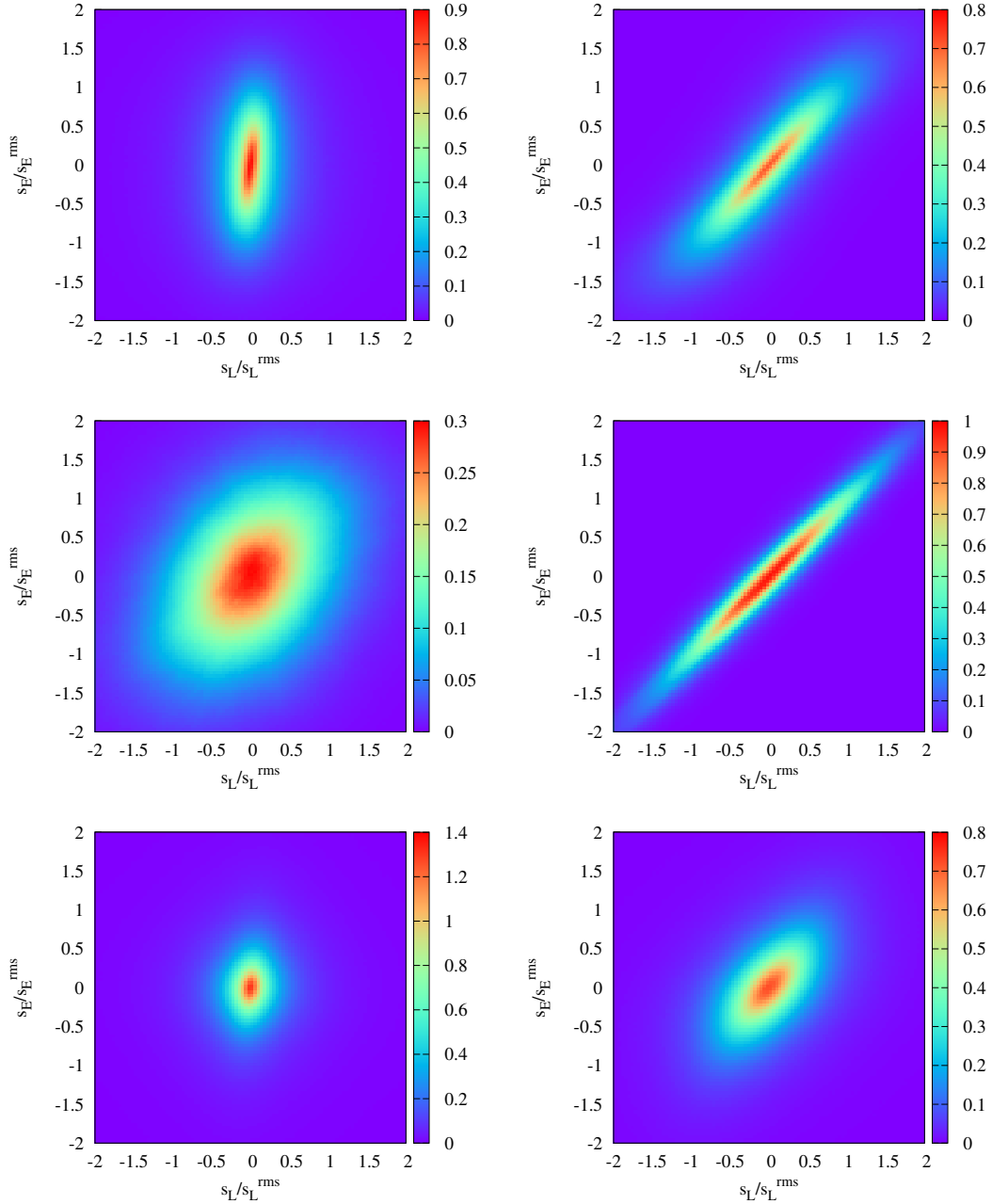


Figure 4. Joint pdfs of Lagrangian time-rate of change of fluctuating density  $\mathbf{s}_L$  and Eulerian time-rate of change of fluctuating density  $\mathbf{s}_E$  for Richardson numbers  $Ri = 0.1$  (left) and  $Ri = 1$  (right) for the total time-rates of change (top), at scale index  $j = 3$  (center), and at scale index  $j = 7$  (bottom) at nondimensional time  $St = 10$ .

cient decreases with increasing scale index  $j$  or decreasing scale of motion.

## SUMMARY

The present study considers the correlations between Lagrangian and Eulerian accelerations and Lagrangian and Eulerian time-rates of change of fluctuating density. The analyses are based on direct numerical simulation data of homogeneous turbulence in stratified shear flows and are an extension of the work presented in Jacobitz *et al.* (2015). The correlations between the accelerations and time-rates of changes are increasing with increasing stratification strength. This increase is due to a diminished importance of the corresponding advection terms in the

Navier–Stokes equation and the advection-diffusion equation for fluctuating density. Since the Lagrangian time-rate of change of fluctuating density is unaffected by a quadratic term, the joint pdf of the time-rates differs from that of the accelerations in the case of weak stratification.

A wavelet-based scale-dependent decomposition of the accelerations and time-rates of change of fluctuating density allows an extension of this analysis to different scales of motion. It was observed that the correlation coefficients increase at every scale of motion with increasing stratification strength. In addition, the correlation coefficients decrease with decreasing scale of motion at every stratification strength considered.

Table 1. Pearson product-moment correlation coefficients  $r$  for Lagrangian acceleration  $\mathbf{a}_L$  and Eulerian acceleration  $\mathbf{a}_E$  at nondimensional time  $St = 10$ . The correlation coefficient is determined for all three components of the accelerations.

$Ri$	0	0.1	0.2	0.5	1	2	5	10
$r$ (total)	0.0284	0.0510	0.0882	0.2852	0.6634	0.8443	0.9067	0.9371
$r$ ( $j = 1$ )	0.8065	0.9347	0.9625	0.9957	0.9990	0.9996	0.9996	0.9998
$r$ ( $j = 3$ )	0.1988	0.3427	0.5072	0.8257	0.9512	0.9732	0.9848	0.9896
$r$ ( $j = 5$ )	0.0308	0.0478	0.0739	0.2002	0.4528	0.5946	0.6614	0.7274
$r$ ( $j = 7$ )	0.0037	0.0097	0.0248	0.1248	0.3337	0.4317	0.4189	0.4136

Table 2. Pearson product-moment correlation coefficients  $r$  for Lagrangian time-rate of change of fluctuating density  $\mathbf{s}_L$  and Eulerian time-rate of change of fluctuating density  $\mathbf{s}_E$  at nondimensional time  $St = 10$ .

$Ri$	0	0.1	0.2	0.5	1	2	5	10
$r$ (total)	0.0219	0.0606	0.1260	0.4034	0.7889	0.9315	0.9747	0.9859
$r$ ( $j = 1$ )	0.7661	0.9165	0.9639	0.9961	0.9995	0.9997	0.9999	1.0000
$r$ ( $j = 3$ )	0.1948	0.3358	0.5145	0.8484	0.9682	0.9890	0.9955	0.9973
$r$ ( $j = 5$ )	0.0379	0.0722	0.1257	0.3171	0.6182	0.7880	0.8683	0.9124
$r$ ( $j = 7$ )	0.0046	0.0258	0.0603	0.2098	0.4067	0.4995	0.5129	0.5318

## ACKNOWLEDGMENTS

FGJ acknowledges the support from an International Opportunity Grant from the University of San Diego and the hospitality at Aix-Marseille Université. KS acknowledges financial support from the ANR, project AIFIT (ANR Grant 15-CE40-0019) and the French Research Federation for Fusion Studies within the framework of the European Fusion Development Agreement (EFDA).

## REFERENCES

- Farge, M. & Schneider, K. 2015 Wavelet transforms and their applications to mhd and plasma turbulence: a review. *J. Plasma Phys.* **81** (6), 435810602.
- Gerz, T., Schumann, U. & Elghobashi, S. E. 1989 Direct numerical simulation of stratified homogeneous turbulent shear flows. *J. Fluid Mech.* **200**, 563–594.
- Hanazaki, H. & Hunt, J. C. R. 2004 Structure of unsteady stably stratified turbulence with mean shear. *J. Fluid Mech.* **507**, 1–42.
- Heisenberg, W. 1948 Zur statistischen theorie der turbulenz. *Zeitschrift für Physik* **124**, 628–657.
- Holt, S. E., Koseff, J. R. & Ferziger, J. H. 1992 A numerical study of the evolution and structure of homogeneous stably stratified sheared turbulence. *J. Fluid Mech.* **237**, 499–539.
- Jacobitz, F. G. 2002 A comparison of the turbulence evolution in a stratified fluid with vertical or horizontal shear. *J. Turbul.* **3**, 1–16.
- Jacobitz, F. G., Sarkar, S. & Van Atta, C. W. 1997 Direct numerical simulations of the turbulence evolution in a uniformly sheared and stably stratified flow. *J. Fluid Mech.* **342**, 231–261.
- Jacobitz, F. G., Schneider, K. & Farge, M. 2015 On acceleration statistics in turbulent stratified shear flows. In *Proceedings of the 9th International Symposium on Turbulence and Shear Flow Phenomena*. Melbourne, Australia.
- Keller, K. H. & Van Atta, C. W. 2000 An experimental investigation of the vertical temperature structure of homogeneous stratified shear turbulence. *J. Fluid Mech.* **425**, 1–29.
- Komori, S., Ueda, H., Ogino, F. & Mizushima, T. 1983 Turbulence structure in stably stratified open-channel flow. *J. Fluid Mech.* **130**, 13–26.
- La Porta, A., Voth, G. A., Crawford, A. M., Alexander, J. & Bodenschatz, E. 2001 Fluid particle accelerations in fully developed turbulence. *Nature* **409**, 1017.
- Mallat, S. 1998 *A Wavelet Tour of Signal Processing*. Academic Press.
- Pope, S. B. 1994 Lagrangian pdf methods for turbulent flows. *Annu. Rev. Fluid Mech.* **26**, 23–63.
- Rogallo, R. S. 1981 Numerical experiments in homogeneous turbulence. Technical Report TM 81315. NASA Ames Research Center, Moffett Field, CA, United States.
- Rohr, J. J., Itsweire, E. C., Helland, K. N. & Van Atta, C. W. 1988 Growth and decay of turbulence in a stably stratified shear flow. *J. Fluid Mech.* **195**, 77–111.
- Toschi, F. & Bodenschatz, E. 2009 Lagrangian properties of particles in turbulence. *Annu. Rev. Fluid Mech.* **41**, 375.
- Tsinober, A. 2001 *An informal introduction to turbulence*. Kluwer Academic Publishers.
- Yeung, P. K. 2002 Lagrangian investigations of turbulence. *Annu. Rev. Fluid Mech.* **34**, 115.